Research Article

Epitaxial Piezoelectric Pb(Zr$_{0.2}$Ti$_{0.8}$)O$_3$ Thin Films on Silicon for Energy Harvesting Devices

A. Sambri,[1, 2] D. Isarakorn,[3] A. Torres-Pardo,[4] S. Gariglio,[1] Pattanaphong Janphuang,[3] D. Briand,[3] O. Stéphan,[4] J. W. Reiner,[5] J.-M. Triscone,[1] Nico F. de Rooij,[3] and C. H. Ahn[5]

[1] *Department of Condensed Matter Physics, (DPMC), University of Geneva, 24 Quai Ernest-Ansermet, 1211 Geneva 4, Switzerland*

[2] *Dipartimento di Scienze Fisiche & CNR-SPIN, Università degli Studi di Napoli Federico II, Complesso Universitario di Monte S. Angelo, Via Cintia, 80126 Napoli, Italy*

[3] *The Sensors, Actuators and Microsystems Laboratory, Institute of Microengineering (IMT), Ecole Polytechnique Fédérale de Lausanne (EPFL), Rue Jaquet-Droz 1, P.O. Box 526, 2002 Neuchâtel, Switzerland*

[4] *Laboratoire de Physique des Solides, Université Paris-Sud, CNRS-UMR 8502, 91405 Orsay, France*

[5] *Department of Applied Physics, Yale University, P.O. Box 208284, New Haven, CT 06520-8284, USA*

Correspondence should be addressed to A. Sambri, sambri@fisica.unina.it

We report on the properties of ferroelectric Pb(Zr$_{0.2}$Ti$_{0.8}$)O$_3$ (PZT) thin films grown epitaxially on (001) silicon and on the performance of such heterostructures for microfabricated piezoelectric energy harvesters. In the first part of the paper, we investigate the epitaxial stacks through transmission electron microscopy and piezoelectric force microscopy studies to characterize in detail their crystalline structure. In the second part of the paper, we present the electrical characteristics of piezoelectric cantilevers based on these epitaxial PZT films. The performance of such cantilevers as vibration energy transducers is compared with other piezoelectric harvesters and indicates the potential of the epitaxial approach in the field of energy harvesting devices.

1. Introduction

In the last decade, studies on epitaxial ferroelectric thin films have led to many interesting results and exciting discoveries [1]. The possibility of tailoring or even enhancing some physical parameters via epitaxial strain engineering [2–4] has suggested the idea of the exploitation of such thin films for several technological applications [5]. Nevertheless, the benefits of the epitaxial approach on the performances of ferroelectric thin film-based devices have to compensate the hurdles related to the epitaxial growth on industrial substrates such as silicon, the modern technological platform. It is in fact well known that the basic requirements for the epitaxy, that is, a good lattice match between substrate and film and a reciprocal chemical stability, are not easily fulfilled in the case of oxide growth on silicon. Beside the difference in lattice parameters and thermal expansion coefficients, the main problem is the surface reactivity of silicon to oxygen,

with the formation of an amorphous layer of silicon dioxide that hints any further epitaxy. Moreover, the cations of most ferroelectric compounds interdiffuse into the silicon substrate, forming spurious extra phases at the interface [6]. In order to overcome such difficulties, a suitable buffer layer is needed that acts as a barrier for cations migration and as a structural template for the growth of the ferroelectric epitaxial film [7–9].

PZT is one of the most investigated ferroelectric materials, due to its high values of remnant polarization and piezoelectric coefficients. In the bulk form, it displays a complex phase diagram versus the Ti/Zr content: for the stoichiometry of our choice, that is, Pb(Zr$_{0.2}$Ti$_{0.8}$)O$_3$ (PZT 20/80), it is ferroelectric with a tetragonal structure up to a transition temperature of 460°C [10]. It is worth stressing that for ferroelectric materials the mechanical boundary conditions may affect substantially the ferroelectric properties because of the strong strain-polarization coupling present in these

compounds [11–13]. Thus, the epitaxial strain often makes the properties of ferroelectric thin films substantially different from the bulk counterpart.

2. Heterostructure Growth and Characterization

The investigated epitaxial heterostructure is composed of a ferroelectric PZT layer grown on top of a metallic $SrRuO_3$ (SRO) film, used as bottom electrode. This bilayer is deposited onto a thin $SrTiO_3$ (STO) film epitaxially grown on a 2-inch (001) silicon wafer. The choice of STO as buffer layer is determined by the fact that it has the same crystalline structure (perovskite) and a good lattice match with SRO and PZT. STO also acts as a barrier for Pb diffusion into the silicon wafer [14–16]. The STO layer can reach a very high degree of crystalline perfection on silicon when the growth is performed by molecular beam epitaxy through a complex multistep process, where fixed amounts of the elemental materials have to be carefully deposited at specific conditions of substrate temperature and pressure. The deposition process we used is detailed in [17, 18]. *In situ* Reflection High Energy Electron Diffraction (RHEED) is the key tool in order to monitor and control the whole deposition procedure, since every step of the deposition corresponds to a specific diffraction pattern linked to a particular surface reconstruction. Figure 1 shows the evolution of the RHEED pattern during the growth of a STO film on silicon.

The SRO and PZT layers are subsequently grown by rf magnetron sputtering as described in [19]. In the following, a detailed investigation of the crystalline structure of a PZT(100 nm)/SRO(30 nm)/STO(6 nm)/Si stack is given. X-ray structural characterization of the heterostructure has been performed with a high-resolution PANalytical X'Pert diffractometer, equipped with a four-bounce asymmetric Ge(220) monochromator for Cu $K\alpha_1$ radiation. Through θ-2θ and ϕ-scan diffractograms, the following out-of-plane orientation and cube-on-cube arrangement of the oxides stack on silicon have been determined: PZT[001]//SRO[001]//STO[001]//Si[001] and PZT [100]//SRO[100]//STO[100]//Si[110] (see also [13]).

Transmission electron microscopy (TEM) characterization, performed on a JEOL JEM2010 microscope, shows at the silicon-STO interface the presence of an amorphous layer of SiO_2, which clearly did not affect the epitaxy of the oxides multilayer (Figure 2).

Most likely then, the formation of this SiO_2 layer occurs after the growth of the STO/Si interface template through oxygen diffusion, thus not hindering the epitaxy [20–22].

Interestingly, the TEM investigation also revealed the presence in the PZT layer of crystallographic domains with the c-axis aligned in the plane of the film, so-called a-domains. Figure 3 shows that their width is about 20 nm. We note that the overlap of the more intense (00l) SRO reflections with the diffraction peaks of the PZT a-domains most probably prevents their detection in the X-ray θ-2θ scans. The origin of the formation of these domains can be related to the strain arising from the lattice and thermal mismatch

of the film with the substrate during the cool-down across the ferroelectric transition [23, 24]. Figure 3(a) shows a pattern of domains in the PZT layer: they repeat periodically every ~105 nm. The domain wall between a and c domains runs along the diagonal of the tetragonal unit cell and the difference between the a and c axis (c/a = 1.046) [13] gives rise to a distortion of the neighboring lattices on each side of a 90° domain wall. The misalignment of the growth planes between a and c domains is clearly visible in Figure 3(c) and can be estimated to be ~3°, in good agreement with the calculated value of ~2.6°.

Due to the different polarization orientations of the c and a domains, respectively, perpendicular and parallel to the film-substrate interface, we can detect their presence by piezoelectric force microscopy (PFM). In PFM, a conducting tip is scanned in contact with the surface while an ac voltage, lower than the coercive field of the material, is applied between the tip and the sample. From the detection of the in-phase and out-of-phase deformation signals in the vertical (V) and lateral (L) PFM modes [25], it is possible to map the presence of a and c domains.

Figure 4(a) shows a topography scan of a PZT surface, revealing a nRMS roughness of 5 nm. The V-PFM scan shown in the middle panel is sensitive to the polarization direction of the c-domains of the film, here shown as reddish area, while the yellowish lines correspond to a-domains, with zero contrast. Conversely, through L-PFM it is possible to detect the piezoelectric response of a-domains, with the restriction that domains parallel to the scan direction cannot be detected, as clearly shown in Figure 4(c). Combining the V-PFM and L-PFM measurements, the PZT film appears to be a very dense network of small a-domains embedded in a matrix of c-axis domains. As can be seen, the phase response detected in the V-PFM and L-PFM is unrelated to the topographic features detected simultaneously by the AFM scan. Figure 5 shows a detail of the PZT a-domains network, on a $1 \times 1 \mu m^2$ area.

According to some reports, applying an electric field induces a lateral motion of thin a-domains [26–33]. Even though some of these results are still under debate, such a motion would give rise to an extrinsic contribution to the piezoelectric response of the material and an enhancement of the conversion coefficients. a-domains switching would indirectly enhance the strain state in the film and its piezoelectric response. Indeed, while the estimation of the PZT d_{33} coefficient by PFM measurement yields a value of about 50 pm/V (in agreement with the data reported for bulk PZT 20/80), the indirect estimation of d_{31} from the deflection of a microfabricated piezoelectric cantilever gives a higher value (details in the next section).

We investigated the ferroelectric behavior of these epitaxial films grown on silicon through a series of polarization hysteresis measurements, performed by a TF analyzer 2000. To perform the measurements, Cr/Au top electrodes were prepared with a size of $100 \times 100 \mu m^2$. The polarization versus voltage loop, shown in Figure 6(a), reveals a remnant polarization of about $70 \mu C \, cm^{-2}$ and no significant leakage current up to 16 V. Figure 6(b) displays the measurement of the capacitance versus applied bias, revealing the dielectric
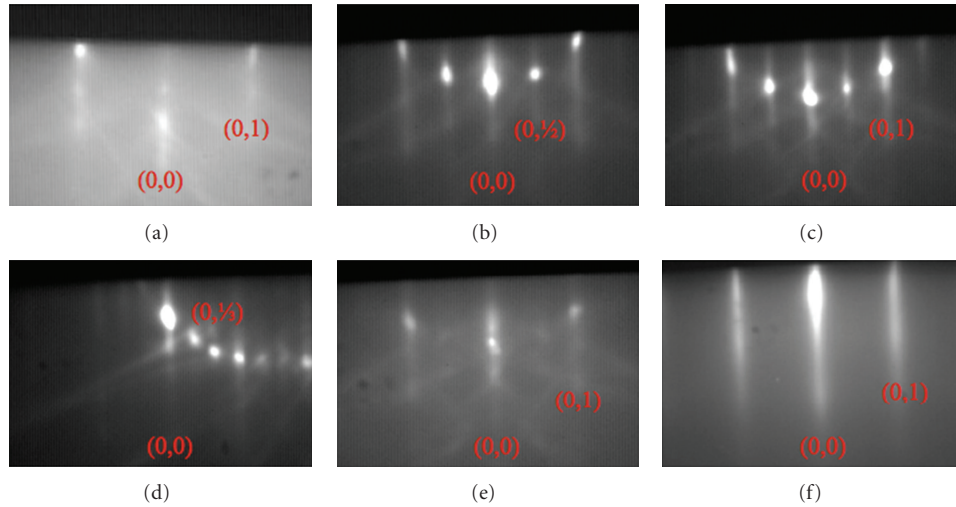
FIGURE 1: Evolution of RHEED pattern during the growth of a STO layer. The patterns shown are taken with the electron beam along the [100] direction. (a) As-received Si wafer (001), the diffuse background indicates the presence of a native amorphous layer of SiO_2; (b) crystalline Si surface after a thermal treatment in vacuum: the appearance of fractional spots (0,1/2) due to Si dimers indicates the complete removal of SiO_2, (c) 2× surface reconstruction corresponding to the deposition of half monolayer (ML) of Sr in vacuum at high temperature, (d) 3× reconstruction corresponding to the deposition of half ML of Sr in vacuum at low temperature, (e) 1 ML of SrO, (f) 3 ML of crystalline STO.
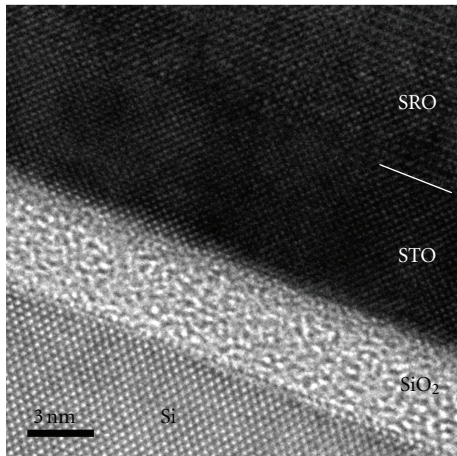

FIGURE 2: Cross-sectional TEM image, revealing the presence of 4.5 nm of amorphous SiO_2 located between the silicon substrate and the epitaxial oxide stack.

FIGURE 3: (a) Cross-sectional TEM image, revealing the presence of periodic a-domains, (b) HRTEM of a single a-domain surrounded by a c-axis oriented regions. (c) Details of the 90° domain wall.

tunability of our epitaxial PZT. In the approximation of a plane capacitor, we estimate a dielectric constant at zero field to be about 150.

3. Energy Harvesting Devices

The development of transducers allowing energy from mechanical vibrations to be generated has advanced rapidly during the past few years. Several review articles [34, 35] discuss the principles and advantages of each conversion method. Among these, piezoelectricity based devices have received large att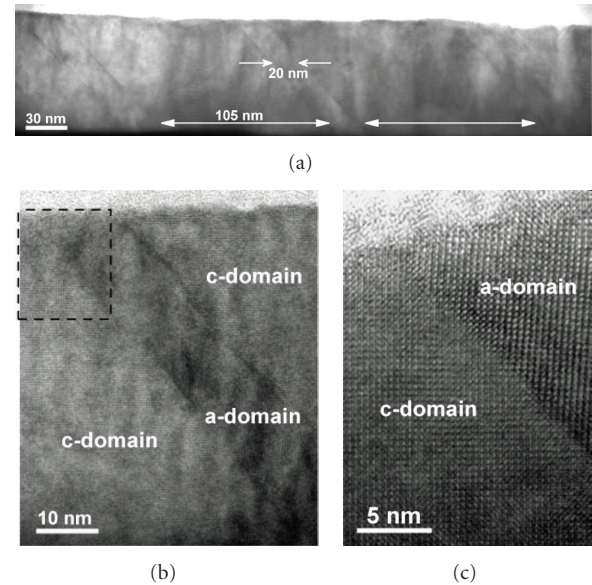ention due to their high power density and ease of integration compared to other transduction techniques [36–38]. Several piezoelectric silicon micromachined energy scavengers have been proposed so far, most of these devices being based on polycrystalline PZT (poly-PZT) or aluminum nitride (AlN) films. Energy harvesting devices involving epitaxial PZT thin films are however less common [39–41]. In this study we report on the characteristics of
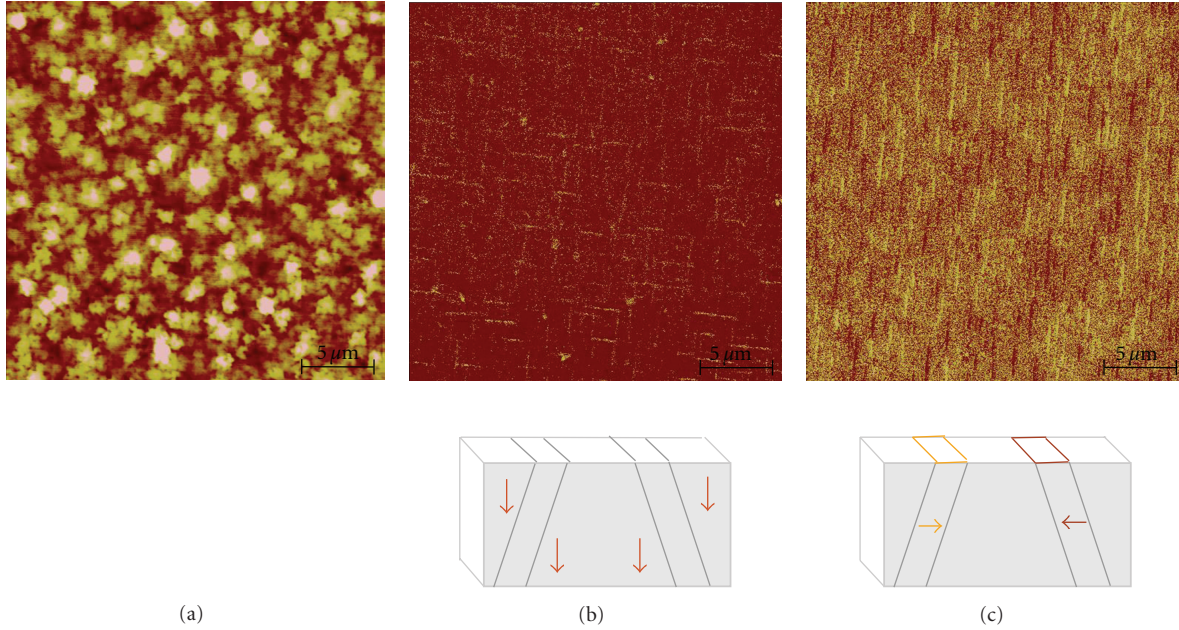
(a)   (b)   (c)

Figure 4: (a) Topography scan on a $20 \times 20\,\mu m^2$ area, (b) V-PFM and (c) L-PFM: phase response of the vertical and lateral PFM measurements on the same area and schematic of the corresponding detected domains.
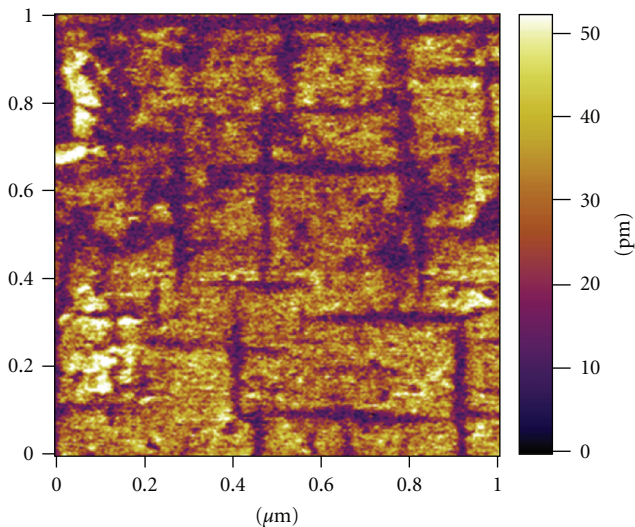

Figure 5: V-PFM scan on a $1 \times 1\,\mu m^2$ area: zoom of the a-domains network.

MEMS based vibrations energy scavengers made of an epitaxial PZT film on silicon cantilevers.

A typical device is shown in Figure 7: it is based on a cantilever fabricated using micropatterning techniques optimized for the oxide layers deposited on silicon. The details of the microfabrication process are presented in [19].

The d_{31} piezoelectric coefficient has been estimated from the displacement at the free end of a cantilever. The deflection of this cantilever, coated with 100 nm thick epi-PZT films, has been measured as a function of dc voltage using an interferometric profiler (Wyko NT110). The piezoelectric

coefficient value is estimated to be 135.4 ± 7.1 pm/V [19]. For a PZT thickness of about 500 nm, we measure a residual stress after the film growth of about 60 MPa, according to stress measurement performed using a Tencor FLX-2320A system. In order to evaluate the performance of our device, the cantilever's resonant frequency has been determined using a Polytec MVS-400 laser Doppler vibrometer, obtaining a value of 2.3 ± 0.1 kHz. The power generation performance of the device has been investigated with a shaker (Bruel and Kjaer type 4811) driven by a vibration exciter control (type 1050) and a power amplifier (type 2712) by applying an acceleration as a mechanical input. The device is connected with various resistive loads (R_L) and the current generated under different acceleration levels is recorded with a multimeter (Agilent 34411A). The corresponding average power is calculated by the relation: $P_{ave} = I_{rms}^2 R_L$. The output current, average power, and voltage as a function of resistive loads are shown in Figure 8.

In order to compare this performance with other MEMS energy harvesters, these output data are normalized as following: the output power per square acceleration (g^2), the current and voltage per acceleration (g). From a single device with an optimal resistive load of 4.7 kΩ, a maximum output power of $14\,\mu W/g^2$ with $60\,\mu A/g$ output current is obtained, thus resulting in an output voltage of 0.28 V/g. The maximum power density is as high as $105\,\mu W/(g^2\,mm^3)$. As shown in details in [41], the comparison of the electrical output characteristics between this epitaxial-PZT energy harvester and other piezo-harvesting devices based on poly-PZT and AlN films [42–46] shows that the former provides higher current at smaller resistive load. Usually, energy harvesting devices with a low optimal load resistance are highly desirable because they can generate high output current,
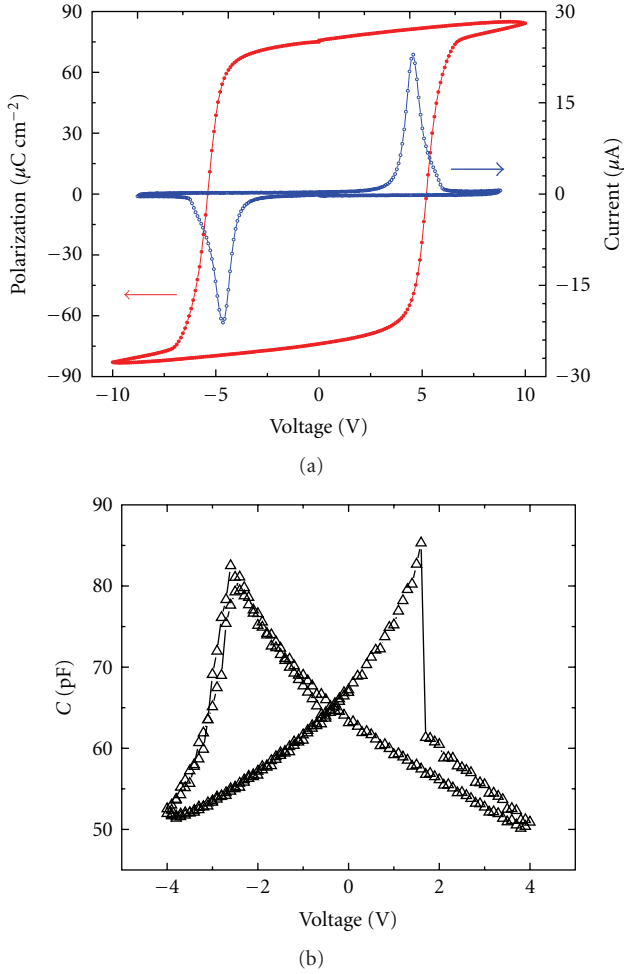
(a)

(b)

Figure 6: (a) Polarization versus applied voltage (PE loop) (full red circle) and corresponding switching current (empty blue circle). (b) Plot of the capacitance versus applied bias. The difference in the coercive field in the PE loop measurement and in the capacitance cycle is due to a different electrical configuration, top-top contacts for PE loos while top-bottom for the capacitance.
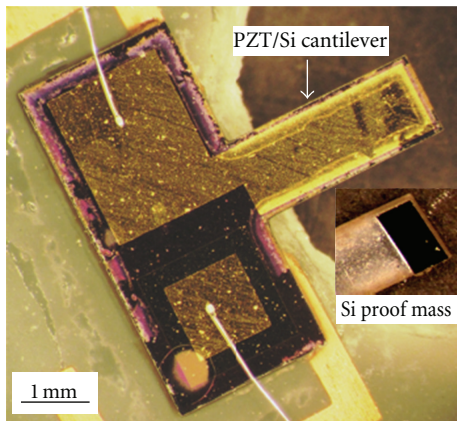

(a)

(b)

(c)

Figure 8: (a) Average power, (b) output current, and (c) corresponding output voltage of an epi-PZT harvester versus resistive load.

Figure 7: Optical image of an epi-PZT cantilever ($1000 \times 2500 \times 7\,\mu m^3$) with a Si proof mass ($1000 \times 500 \times 230\,\mu m^3$). The inset shows the Si proof mass on the back side of the cantilever. The effective volume of the final device is $0.1325\,mm^3$.
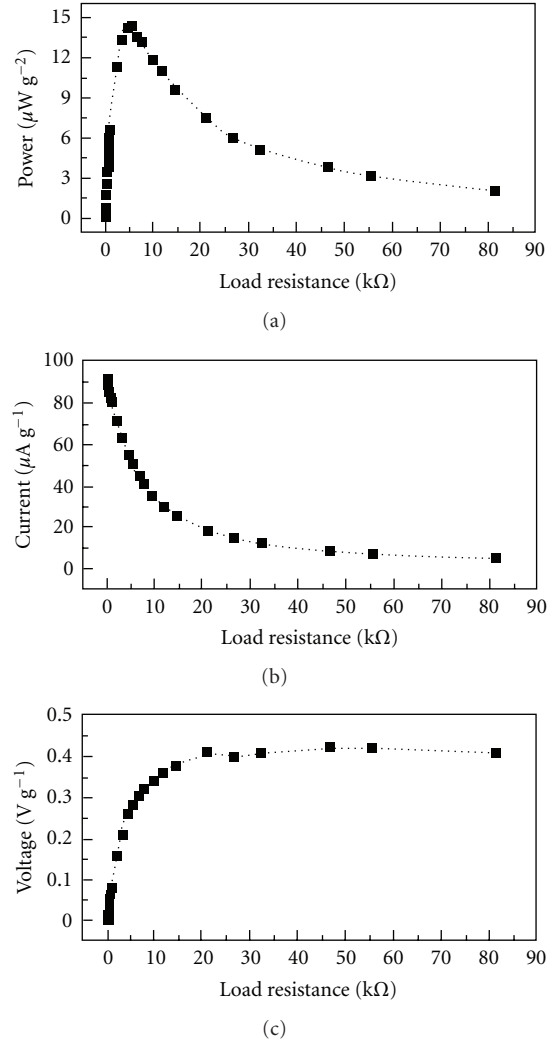
and also because their impedance can be easily matched to standard electronic devices. Energy harvesting devices based on poly-PZT and AlN films demonstrated useful power generation, but their high impedance limits the output current. Moreover, even though the power generated by the epi-PZT is similar to that of AlN, the epi-PZT harvester exhibits the highest power density, which is of high interest when realizing miniaturized devices. Unlike the polycrystalline film based devices, the device reported here can generate high power and current with usable voltage, while maintaining low optimal resistive load. For piezoelectric energy harvesters, the expressions for the figure of merit for the power, voltage and current are, respectively: $P_F = e_{31,f}^2/\epsilon_r$, $V_F = e_{31,f}/\epsilon_r$, $I_F = e_{31,f}^2$, where $e_{31,f}$ is the effective piezoelectric coefficient. From the measured piezoelectric coefficient d_{31}, it is possible to estimate a value of $18.2 \pm 0.9\,C\,m^{-2}$ [47], a value which is significantly higher than what has been reported in the past [48]. Such large piezoelectric coefficient

together with a low dielectric constant is among the key parameters to realize high performance piezoelectric energy harvesters.

4. Conclusions

This paper reports on the structural and physical properties of epitaxial PZT thin films deposited on silicon and on the electrical performance of cantilevers microfabricated from such heterostructures. We have shown that the PZT thin films exhibit excellent ferroelectric characteristics with a remnant polarization of $70\,\mu C\,cm^{-2}$. The structural microscopic investigation by TEM and PFM has revealed the presence of a-domains embedded in a mostly oriented c-axis film. This coexistence of domains with different crystallographic orientation could be at the origin of the large piezoelectric response estimated from the electromechanical behavior of the cantilevers. The performances of our epitaxial piezo-transducers fabricated for energy harvesting indicate that these generate higher power and current with usable voltage requiring lower optimal resistive load as compared to piezoelectric harvesters realized with polycrystalline PZT or AlN films.

Acknowledgments

References

[1] M. Dawber, K. M. Rabe, and J. F. Scott, "Physics of thin-film ferroelectric oxides," *Reviews of Modern Physics*, vol. 77, no. 4, pp. 1083–1130, 2005.

[2] J. H. Haeni, P. Irvin, W. Chang et al., "Room-temperature ferroelectricity in strained $SrTiO_3$," *Nature*, vol. 430, no. 7001, pp. 758–761, 2004.

[3] K. J. Choi, M. Biegalski, Y. L. Li et al., "Enhancement of ferroelectricity in strained $BaTiO_3$ thin films," *Science*, vol. 306, no. 5698, pp. 1005–1009, 2004.

[4] P. Zubko, N. Stucki, C. Lichtensteiger, and J. M. Triscone, "X-ray diffraction studies of $180°$ ferroelectric domains in $PbTiO_3/SrTiO_3$ superlattices under an applied electric field," *Physical Review Letters*, vol. 104, no. 18, Article ID 187601, 2010.

[5] N. Setter, D. Damjanovic, L. Eng et al., "Ferroelectric thin films: Review of materials, properties, and applications," *Journal of Applied Physics*, vol. 100, no. 10, Article ID 109901, 2006.

[6] P. Revesz, J. Li, N. Szabo Jr., W. Mayer, D. Caudillo, and E. R. Myers, "PZT interaction with metals and oxides studied by RBS," *Materials Research Society Symposium Proceedings*, vol. 243, pp. 101–106, 1991.

[7] R. A. McKee, F. J. Walker, and M. F. Chisholm, "Crystalline oxides on silicon: the first five monolayers," *Physical Review Letters*, vol. 81, no. 14, pp. 3014–3017, 1998.

[8] J. W. Reiner, A. M. Kolpak, Y. Segal et al., "Crystalline oxides on silicon," *Advanced Materials*, vol. 22, no. 26–27, pp. 2919–2938, 2010.

[9] Z. Yu, Y. Liang, C. Overgaard et al., "Advances in heteroepitaxy of oxides on silicon," *Thin Solid Films*, vol. 462-463, pp. 51–56, 2004.

[10] B. Jaffe, W. R. Cook, and H. Jaffe, *Piezoelectric Ceramics*, Academic Press, London, UK, 1971.

[11] N. A. Pertsev, A. G. Zembilgotov, and A. K. Tagantsev, "Effect of mechanical boundary conditions on phase diagrams of epitaxial ferroelectric thin films," *Physical Review Letters*, vol. 80, no. 9, pp. 1988–1991, 1998.

[12] D. G. Schlom, L. Q. Chen, C. B. Eom, K. M. Rabe, S. K. Streiffer, and J. M. Triscone, "Strain tuning of ferroelectric thin films," *Annual Review of Materials Research*, vol. 37, pp. 589–626, 2007.

[13] A. Sambri, S. Gariglio, A. Torres Pardo et al., "Enhanced critical temperature in epitaxial ferroelectric Pb $(Zr_{0.2}Ti_{0.8})$ O_3 thin films on silicon," *Applied Physics Letters*, vol. 98, no. 1, Article ID 012903, 3 pages, 2011.

[14] D. S. Shin, S. T. Park, H. S. Choi, I. H. Choi, and J. Y. Lee, "Characteristics of $Pt/SrTiO_3/Pb(Zr_{0.52},\ Ti_{0.48})O_3/SrTiO_3/Si$ ferroelectric gate oxide structure," *Thin Solid Films*, vol. 354, no. 1, pp. 251–255, 1999.

[15] Ø. Nordseth, C. C. You, E. Folven et al., "Growth and characterization of $(Pb,La)(Zr,Ti)O_3$ thin film epilayers on $SrTiO_3$-buffered Si(001)," *Thin Solid Films*, vol. 518, no. 19, pp. 5471–5477, 2010.

[16] E. Tokumitsu, K. Itani, B. K. Moon, and H. Ishiwara, "Crystalline quality and electrical properties of $PbZr_xTi_{1-x}O_3$ thin films prepared on $SrTiO_3$-covered Si substrates," *Japanese Journal of Applied Physics*, vol. 34, no. 9, pp. 5202–5206, 1995.

[17] J. W. Reiner, K. F. Garrity, F. J. Walker, S. Ismail-Beigi, and C. H. Ahn, "Role of strontium in oxide epitaxy on silicon (001)," *Physical Review Letters*, vol. 101, no. 10, Article ID 105503, 2008.

[18] J. Lettieri, J. H. Haeni, and D. G. Schlom, "Critical issues in the heteroepitaxial growth of alkaline-earth oxides on silicon," *Journal of Vacuum Science and Technology A*, vol. 20, no. 4, pp. 1332–1340, 2002.

[19] D. Isarakorn, A. Sambri, P. Janphuang et al., "Epitaxial piezoelectric MEMS on silicon," *Journal of Micromechanics and Microengineering*, vol. 20, no. 5, Article ID 055008, 2010.

[20] G. J. Norga, C. Marchiori, C. Rossel et al., "Solid phase epitaxy of $SrTi\ O_3$ on $(Ba,Sr)O/Si(100)$: the relationship between oxygen stoichiometry and interface stability," *Journal of Applied Physics*, vol. 99, no. 8, Article ID 084102, 7 pages, 2006.

[21] L. V. Goncharova, D. G. Starodub, E. Garfunkel et al., "Interface structure and thermal stability of epitaxial $SrTiO_3$ thin films on Si(001)," *Journal of Applied Physics*, vol. 100, no. 1, Article ID 014912, 2006.

[22] V. Shutthanandan, S. Thevuthasan, Y. Liang, E. M. Adams, Z. Yu, and R. Droopad, "Direct observation of atomic disordering at the $SrTiO_3/Si$ interface due to oxygen diffusion," *Applied Physics Letters*, vol. 80, no. 10, Article ID 1803, 3 pages, 2002.

[23] J. S. Speck and W. Pompe, "Domain configurations due to multiple misfit relaxation mechanisms in epitaxial ferroelectric thin films. I. Theory," *Journal of Applied Physics*, vol. 76, no. 1, pp. 466–476, 1994.

[24] B. S. Kwak, A. Erbil, J. D. Budai, M. F. Chisholm, L. A. Boatner, and B. J. Wilkens, "Domain formation and strain relaxation in epitaxial ferroelectric heterostructures," *Physical Review B*, vol. 49, no. 21, pp. 14865–14879, 1994.

[25] S. V. Kalinin, B. J. Rodriguez, S. Jesse et al., "Vector piezoresponse force microscopy," *Microscopy and Microanalysis*, vol. 12, no. 3, pp. 206–220, 2006.

[26] Z. Ma, F. Zavaliche, L. Chen et al., "Effect of 90° domain movement on the piezoelectric response of patterned $PbZr_{0.2}Ti_{0.8}O_3/SrTiO_3$ Si heterostructures," *Applied Physics Letters*, vol. 87, no. 7, Article ID 072907, 3 pages, 2005.

[27] N. Bassiri-Gharb, I. Fujii, E. Hong, S. Trolier-Mckinstry, D. V. Taylor, and D. Damjanovic, "Domain wall contributions to the properties of piezoelectric thin films," *Journal of Electroceramics*, vol. 19, no. 1, pp. 47–65, 2007.

[28] G. Le Rhun, I. Vrejoiu, L. Pintilie, D. Hesse, M. Alexe, and U. Gösele, "Increased ferroelastic domain mobility in ferroelectric thin films and its use in nano-patterned capacitors," *Nanotechnology*, vol. 17, no. 13, article 013, pp. 3154–3159, 2006.

[29] V. Nagarajan, A. Roytburd, A. Stanishevsky et al., "Dynamics of ferroelastic domains in ferroelectric thin films," *Nature Materials*, vol. 2, no. 1, pp. 43–47, 2003.

[30] R. J. Zednik, A. Varatharajan, M. Oliver, N. Valanoor, and P. C. McIntyre, "Mobile ferroelastic domain walls in nanocrystalline PZT films: the direct piezoelectric effect," *Advanced Functional Materials*, vol. 21, no. 16, pp. 3104–3110, 2011.

[31] I. Vrejoiu, G. Le Rhun, L. Pintilie, D. Hesse, M. Alexe, and U. Gösele, "Intrinsic ferroelectric properties of strained tetragonal $PbZr_{0.2}Ti_{0.8}O_3$ obtained on layer-by-layer grown, defect-free single-crystalline films," *Advanced Materials*, vol. 18, no. 13, pp. 1657–1661, 2006.

[32] L. J. Klein, C. Dubourdieu, M. M. Frank, J. Hoffman, J. W. Reiner, and C. H. Ahn, "Domain dynamics in epitaxial Pb$(Zr_{0.2}Ti_{0.8})O_3$ films studied by piezoelectric force microscopy," *Journal of Vacuum Science and Technology B*, vol. 28, no. 4, article C5A20, 4 pages, 2010.

[33] H. Morioka, K. Saito, H. Nakaki, R. Ikariyama, T. Kurosawa, and H. Funakubo, "Impact of 90°-domain wall motion in $Pb(Zr_{0.43}Ti_{0.57})O_3$ film on the ferroelectricity induced by an applied electric field," *Applied Physics Express*, vol. 2, no. 4, Article ID 041401, 3 pages, 2009.

[34] S. P. Beeby, M. J. Tudor, and N. M. White, "Energy harvesting vibration sources for microsystems applications," *Measurement Science and Technology*, vol. 17, no. 12, pp. R175–R195, 2006.

[35] P. D. Mitcheson, E. K. Reilly, T. Toh, P. K. Wright, E. M. Yeatman, and J. Micromech, "Performance limits of the three MEMS inertial energy generator transduction types," *Journal of Micromechanics and Microengineering*, vol. 17, supplement 9, pp. S211–S216, 2007.

[36] S. R. Anton and H. A. Sodano, "A review of power harvesting using piezoelectric materials (2003–2006)," *Smart Materials and Structures*, vol. 16, no. 3, article R01, pp. R1–R21, 2007.

[37] S. Roundy and P. K. Wright, "A piezoelectric vibration based generator for wireless electronics," *Smart Materials and Structures*, vol. 13, no. 5, pp. 1131–1142, 2004.

[38] P. Muralt, R. G. Polcawich, and S. Trolier-McKinstry, "Piezoelectric thin films for sensors, actuators, and energy harvesting," *MRS Bulletin*, vol. 34, no. 9, pp. 658–664, 2009.

[39] E. K. Reilly and P. K. Wright, "Modeling, fabrication and stress compensation of an epitaxial thin film piezoelectric microscale energy scavenging device," *Journal of Micromechanics and Microengineering*, vol. 19, no. 9, Article ID 095014, 2009.

[40] T. Harigai, H. Adachi, and E. Fujii, "Vibration energy harvesting using highly (001)-oriented $Pb(Zr,Ti)O_3$ thin film," *Journal of Applied Physics*, vol. 107, no. 9, Article ID 096101, 3 pages, 2010.

[41] D. Isarakorn, D. Briand, P. Janphuang et al., "The realization and performance of vibration energy harvesting MEMS devices based on an epitaxial piezoelectric thin film," *Smart Materials and Structures*, vol. 20, no. 2, Article ID 025015, 2011.

[42] R. Elfrink, T. M. Kamel, M. Goedbloed et al., "Vibration energy harvesting with aluminum nitride-based piezoelectric devices," *Journal of Micromechanics and Microengineering*, vol. 19, no. 9, Article ID 094005, 2009.

[43] Y. B. Jeon, R. Sood, J. H. Jeong, and S. G. Kim, "MEMS power generator with transverse mode thin film PZT," *Sensors and Actuators, A*, vol. 122, no. 1, pp. 16–22, 2005.

[44] B. S. Lee, S. C. Lin, W. J. Wu, X. Y. Wang, P. Z. Chang, and C. K. Lee, "Piezoelectric MEMS generators fabricated with an aerosol deposition PZT thin film," *Journal of Micromechanics and Microengineering*, vol. 19, no. 6, Article ID 065014, 2009.

[45] H.-B. Fang, J.-Q. Liu, Z.-Y. Xu et al., "Fabrication and performance of MEMS-based piezoelectric power generator for vibration energy harvesting," *Microelectronics Journal*, vol. 37, no. 11, pp. 1280–1284, 2006.

[46] D. Shen, J. H. Park, J. Ajitsaria, S. Y. Choe, H. C. Wikle III, and D. J. Kim, "The design, fabrication and evaluation of a MEMS PZT cantilever with an integrated Si proof mass for vibration energy harvesting," *Journal of Micromechanics and Microengineering*, vol. 18, no. 5, Article ID 055017, 2008.

[47] P. Muralt, "Piezoelectric thin film for MEMS," *Integrated Ferroelectrics*, vol. 17, no. 1, pp. 297–307, 1997.

[48] S. Trolier-Mckinstry and P. Muralt, "Thin film piezoelectrics for MEMS," *Journal of Electroceramics*, vol. 12, no. 1-2, pp. 7–17, 2004.